ELSEVIER

Journal of Biomechanics 37 (2004) 789–795

JOURNAL OF BIOMECHANICS

www.elsevier.com/locate/jbiomech
www.JBiomech.com

Borelli Lecture from the American Society of Biomechanics Conference 2002

Biomechanics of microscopic appendages: functional shifts caused by changes in speed

M.A.R. Koehl*

Department of Integrative Biology, University of California, Berkeley, CA 94720-3140, USA

Accepted 23 June 2003

Abstract

Many diverse animals use arrays of hair-like structures to perform important jobs such as feeding, gas exchange, smelling, and swimming. Since these functions involve hair interactions with the surrounding water or air, analysis of the fluid dynamics of diverse hair-bearing appendages reveals how the morphology of an array of hairs affects it performance. Mathematical and physical models of flow between cylinders have shown that arrays of large, rapidly moving cylinders are leaky sieves, whereas little fluid moves through a row of small, slow rods. The purpose of the present study was to test this prediction for realistic appendage morphologies and to elucidate whether the design of a hairy leg can affect the range of speeds in which this transition in function occurs. We studied flow through hairy food-capturing appendages (second maxillae) of calanoid copepods, abundant planktonic crustaceans whose feeding on unicellular algae forms an important link in many marine food webs. Using dynamically scaled physical models, we found that hairy appendages undergo a transition between paddle- and sieve-like function at a critical range of sizes and speeds. The coarser the mesh of hairs on second maxillae, the smaller the size and speed at which this functional shift occurs. Thus, a simple increase in size (ontogenetic or evolutionary) or speed can generate a novel function (a paddle can become a filter), but the morphology of a hairy appendage determines the size and speed range at which leakiness to fluid flow can be affected by behavior or growth.

Keywords: Reynolds number; Copepod; Suspension feeding; Setae; Hydrodynamics

1. Introduction

Although most biomechanical research focuses on humans, comparative biomechanics involves analysis of the mechanical design and physical performance of diverse animals, plants, or microorganisms. Many studies in comparative biomechanics map structure and mechanical performance onto phylogenies to investigate the evolution of such traits (e.g. reviewed in Wainwright and Reilly, 1994), while other studies focus on unraveling the basic mechanisms underlying how various organisms perform physical functions (e.g. reviewed in Alexander, 1968; Dickinson et al., 2000; Niklas, 1992; Vogel, 1994; Wainwright et al., 1976). My research in comparative biomechanics falls into the latter category and has had two main thrusts: investigating how organisms interact mechanically with each other and their physical environments (e.g. Koehl, 1999), and studying how the morphology of certain categories of biological structures affects their physical performance (e.g. Koehl, 1996a). The approach I use for such work is to: (1) identify a basic type of structure used widely among diverse types of organisms to perform biologically important physical functions, (2) study the mechanisms underlying how they work, (3) use the diversity of form of such structures among different organisms to sort out how particular aspects of their morphology affect defined aspects of performance, and (4) employ the basic design principles revealed by such research to study how specific organisms function in their natural habitats. In this paper I discuss one of the basic types of biological structures we have been studying using this approach: appendages bearing arrays of filaments.

*Tel.: +1-510-642-8103; fax: +1-510-643-6264.
E-mail address: cnidaria@socrates.berkeley.edu (M.A.R. Koehl).

0021-9290/$ - see front matter © 2003 Elsevier Ltd. All rights reserved.
doi:10.1016/j.jbiomech.2003.06.001

1.1. Appendages bearing arrays of filaments

Many diverse animals use arrays of hair-like structures to perform critical biological functions, from molecule or particle capture (e.g. gills, olfactory antennae, suspension-feeding appendages) to momentum transfer (e.g. swimming legs, ventilatory appendages, wings, flow mechanosensors), that depend on the interaction of the hairs with the surrounding fluid (e.g. Koehl, 1995, 1996b, 1998, 2001a, b; Rubenstein and Koehl, 1977). The pattern of fluid flow around a hair depends on the magnitude of inertial forces relative to viscous forces, as represented by the Reynolds number ($Re = \rho u l/\mu$, where u is velocity, l is hair diameter, and ρ and μ are the density and viscosity, respectively, of the fluid). The fluid in contact with a moving object does not slip relative to the object's surface, hence a velocity gradient develops in the fluid around the structure. The smaller or slower the object (i.e., the lower its *Re*), the thicker this layer of sheared fluid is relative to the size of the structure (e.g. Vogel, 1994; White, 1974). If the layers of sheared fluid moving with the hairs in an array are thick relative to the gaps between hairs, then little fluid leaks through the array, which functions more like a solid paddle than like a porous screen. Mathematical and physical models of flow between cylinders (Cheer and Koehl, 1987a, b; Koehl, 1992, 1995; Loudon et al., 1994) have revealed that a transition between unleaky, paddle-like behavior and leaky, sieve-like function occurs at hair *Re*'s between 10^{-2} and 1. The purpose of the present study was to test this prediction for a realistic appendage morphology and to elucidate whether the design of a hairy leg can affect the *Re* range in which this transition in function occurs.

1.2. Food capture by calanoid copepods

We focused on the food-capturing appendages (second maxillae, M2's) of calanoid copepods (Fig. 1A) to study the effect of the coarseness of an array of filaments on the sensitivity of appendage leakiness to changes in speed or size (i.e. changes in *Re*). Calanoid copepods are small (body length of a few mm's) planktonic crustaceans that are extremely abundant in oceans and lakes. Many copepod species eat single-celled algae suspended in the surrounding water, and are in turn eaten by other animals such as fish. Because copepods form a critical link in aquatic food webs between the primary producers and larger animals, copepod feeding is of great ecological importance (e.g. reviewed in Donaghay, 1988; Frost, 1980; Hansen et al., 1994; Harris, 1996; Kleppel, 1993; Koehl, 1984; Paffenhöfer, 1988; Naganuma, 1996).

High-speed microcinematography of feeding copepods revealed that a pair of M2's capture single-celled algae by "flinging" apart from each other (Fig. 1B) and then "squeezing" back together again (Fig. 1C) (sensu Koehl and Strickler, 1981). Like many hairy appendages (e.g. moth antennae, polychaete gills, crinoid pinnules, barnacle cirri, cladoceran swimming antennae), M2's are composed of large cylinders (setae) that bear smaller cylinders (setules); the coarseness of this mesh of hairs differs between species (e.g. Itoh, 1970; Koehl, 1995) (Fig. 2). Copepod M2's are an ideal system for investigating the effects of morphology on whether changes in appendage kinematics alter the leakiness of hair-bearing appendages, not only because the M2's of various species provide a range of morphological designs to study, but also because their setae operate in the transitional range of *Re*'s between 10^{-2} and 1 (Koehl, 1992, 1995, 2001a; Koehl and Strickler, 1981).

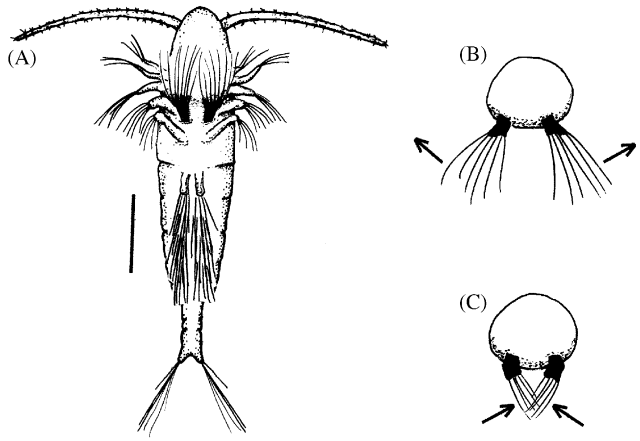

Fig. 1. (A) Diagram of the ventral surface of calanoid copepod (scale bar = 250 μm). The long sensory antennae are at the anterior end of the animal. The anterior setulose appendages produce a feeding current past the animal as it hovers in the water column (Koehl and Strickler, 1981), while the posterior appendages are used for more rapid swimming. The second maxillae (the pair of appendages shown in black), which are located near the animal's mouth, capture food items such as unicellular algae (see Fig. 2 for realistic diagrams of M2's). (B and C). Diagrams of a cross-section of a copepod, showing the second maxillae (M2's) on the ventral surface. During food capture, the M2's first fling apart as indicated by the arrows in (B), and then squeeze back together towards the body surface as shown by the arrows in (C).

2. Methods

2.1. Dynamically scaled physical models

Dynamically scaled physical models were used to study flow through the coarsely meshed M2's of *Centropages velificatus,* the finely meshed M2's of *Temora stylifera,* and the intermediate M2's of *Eucalanus pileatus* (Fig. 2). If a model has the same geometry and *Re* as a real M2, the ratios of the velocities and of

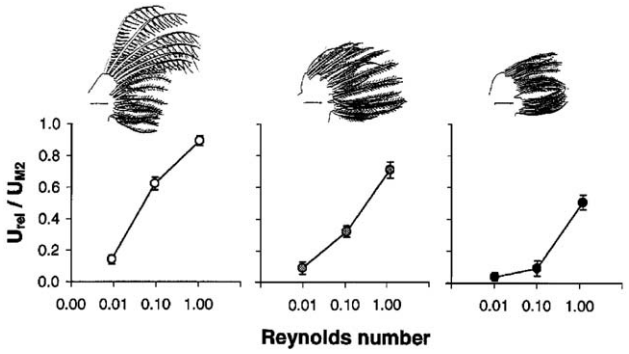

Fig. 2. Mean U_{rel}/U_{M2} for the section of each model $0.25L-0.50L$ from the seta tip (L = seta length), plotted as a function of seta *Re* for models of the M2's of *C. velificatus* (open circles), *E. pileatus* (stippled circles), and *T. stylifera* (black circles). A diagram of a M2 from each species is shown above the graph for that species (scale bar = 50 μm); the large hairs (setae) on the M2's bear smaller hairs (setules). Error bars represent ± one standard deviation (n = 5–12, depending on number of particles visible). These results are consistent with those reported for earlier versions of these models (Koehl, 1995, 1998). There was a significant difference (ANOVA,SNK, $p < 0.05$) between U_{rel}/U_{M2} at different *Re*'s for each species except *T. stylifera,* whose U_{rel}/U_{M2} did not differ significantly between *Re*'s of 10^{-2} and 10^{-1}.

the forces at specific points in the fluid around the model are the same as for analogous points around the prototype M2, i.e. they are dynamically similar (e.g. Vogel, 1994; Koehl, 2003). Large models of M2's were programmed to execute fling-and-squeeze motions slowly in a fluid of high viscosity so that we could quantify the small-scale flow that occurs at the same *Re* through the microscopic real M2's. Such models also enabled us to measure flow through the M2's at *Re*'s not used by the animals.

Physical models (48–57 mm in length) were constructed from sheet metal and precision wire (Small Parts Inc.) that were geometrically similar to the M2's of *C. furcatus, E. pileatus*, and *T. stylifera*. The lengths, diameters, spacings, and angles of the model setae and setules were calculated using means of measurements of these parameters in light micrographs and SEMs of six M2's of adult females of each species (Koehl, unpubl. data). Because the setae on a M2 spread apart from each other during a fling (Koehl and Strickler, 1981; Koehl, 1992) (Fig. 1B), the models were built to mimic the greatest distance attained between setae during a fling-and-squeeze, as measured on high-speed (500 frames/s) movies of feeding copepods (Koehl and Strickler, 1981; Koehl and Paffenhofer, unpubl. data). Each pair of model M2's was mounted on a wall (to simulate the body surface) in a tank (1 m × 1 m × 0.55 m) of mineral oil; a stepping motor (Superior Electric Slo-Syn M091-FD06) rotated the M2's about pivots at their proximal ends to mimic fling-and-squeeze motions of a copepod (Koehl and Strickler, 1981; Koehl and Paffenhofer, unpubl. data). The denisty (ρ) and viscosity (μ) of the mineral oil was measured before each experiment as described by Loudon et al. (1994), and the speed (u) of the M2's at a position 38% of the length of the seta from the tip was adjusted to yield *Re*'s of 1, 10^{-1}, and 10^{-2} (calculated using model seta diameter at this position for l). *E. pileatus* models were also moved at *Re*'s used by the M2's of this species during specific behaviors (described below). Each M2 model swept out and back through an arc of 70°, as they do when capturing single algal cells (Koehl and Strickler, 1981; Koehl, 1995); *E. pileatus* models also swept through arcs of 30° to mimic their small-particle feeding mode (Price et al., 1983; Price and Paffenhöfer, 1984, 1986).

2.2. Analysis of flow through second maxillae

Fiber-optic lamps (Cole Parmer #9741) shining through a slit (1 mm wide) in an aluminum plate on the side of the tank were used to illuminate a plane in the mineral oil parallel to a seta (marked with white dots at its base and tip) in the middle of the row of setae on each M2 model. The fluid was marked with neutrally buoyant particles (*Artemia salina* cysts). Video records were made (Watec WAT-902 CCD video camera, Panasonic AG-7350 VCR) of the motion of the models and the marker particles. The particles and dots on the setae were digitized using a Peak Performance Video Motion Analysis System (version 5.1.0) during the middle 10° of the arc swept by a M2. Five particles that were clearly visible within a distance of $0.2L$ (L = seta length) of the illuminated seta were digitized for 10 frames (1° arc of travel between successive frames digitized), and the mean velocity of each dot and particle was calculated. These data were used to calculate the velocity of the fluid relative to the appendage (U_{rel} = [velocity normal to the seta of a fluid marker particle]—[U_{M2}], where U_{M2} is the velocity of the seta at the position along its length next to the marker particle). For each particle, we calculated U_{rel}/U_{M2} as a measure of the leakiness of the model at that position along the seta. Because we could not control the positions of the marker particles, five separate runs for each model and *Re* were digitized and the data were pooled to provide a distribution of points along the length of the seta. The seta was divided into four sectors of equal length and the mean U_{rel}/U_{M2} for each was calculated.

2.3. Comparison of flow through model and real M2's

How well the hydrodynamics of the real M2's was mimicked by the models was assessed by comparing flow velocities through real M2's ($U_{rel,REAL}$) with those estimated from measurements of flow through model M2's ($U_{rel,EST}$) operating at the same *Re*'s. This

test was done for *E. pileatus*, which have three distinct M2 behaviors: (1) small-particle feeding mode, during which the M2's execute a series of low-amplitude fling-and-squeeze motions (Price and Paffenhöfer, 1984, 1986) ($Re = 2 \times 10^{2}$), (2) capture of individual algal cells ($Re = 8 \times 10^{-2}$), and (3) rejection of unwanted material ($Re = 2 \times 10^{-1}$) (Koehl, 1992, 1995, 2001a; Koehl and Strickler, 1981; Koehl and Paffenhofer, unpubl. data).

High-speed microcinematography was used to record water flow through real M2's of adult female *E. pileatus* performing each of these behaviors. Published procedures were followed for conditioning, handling, and filming (16 mm movies, 500 frames/s) the copeods (Koehl and Strickler, 1981; Price et al., 1983; Price and Paffenhöfer, 1984, 1986), releasing water marked with dye (food coloring) from a micropipette to visualize flow near their M2's (Koehl and Strickler, 1981), and measuring velocities of setae and dye-marked water (Koehl and Strickler, 1981; Koehl, 1995). Ten movies (4000 frames per movie) of each of the feeding behaviors (behaviors #1 and #2) were analyzed, and any rejections (behavior #3) that also occurred in these movies were measured as well. Water velocity through the real M2's ($U_{\mathrm{rel,REAL}}$) was determined for sequences in which a M2 moving in the plane of the film swept through a line of dye. $U_{\mathrm{rel,REAL}}$ was calculated by subtracting the velocity normal to a seta of the leading edge of the line of dye from that seta's velocity ($U_{\mathrm{M2,REAL}}$) at the position of the dye line.

Measurements of mean $U_{\mathrm{rel}}/U_{\mathrm{M2}}$ at four positions (described above) along the models of *E. pileatus* M2's were multiplied by the mean velocities ($U_{\mathrm{M2,REAL}}$) of those positions measured on movies of real *E. pileatus* to estimate the water velocities ($U_{\mathrm{rel,EST}}$) at those positions through the M2's of real *E. pileatus* .

2.4. Statistics

Statistical analyses were done using SigmaStat 2.0 software (Jandel Corp.). Data were tested for equal variance and normal distribution (Kolmogorov–Smirnof test with Lilliefor's correction) before ANOVA and Student–Newman–Keuls (SNK) tests were conducted.

3. Results

3.1. Comparison of flow through model and real second maxillae

The water velocities ($U_{\mathrm{rel,REAL}}$) measured through the M2's of *E. pileatus* were similar to those ($U_{\mathrm{rel,EST}}$) calculated from measurements of fluid flow through the models of the M2's of that species operating at the same *Re* (Fig. 3). This was true for a range of positions along the length of the setae of the M2's, and for three different behaviors used by *E. pileatus*. Thus, the flow produced by our physical models was realistic.

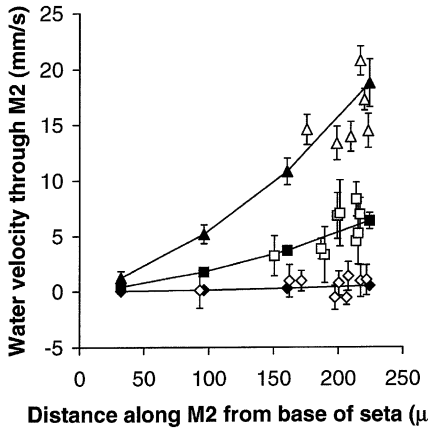

Fig. 3. Water velocity (U_{rel}) through an *E. pileatus* M2, plotted as a function of distance from the proximal ends of the setae, during rejections (triangles), single 70° fling-and-squeeze motions to capture large particles (squares), and one of a series of 30° out-and-in motions to pump water containing small particles towards the mouth (diamonds). Velocities calculated from model $U_{\mathrm{rel}}/U_{\mathrm{M2}}$'s ($U_{\mathrm{rel,EST}}$, black symbols connected by lines) are similar to those calculated from measurements of dye and M2's on movies of real *E. pileatus* ($U_{\mathrm{rel,REAL}}$, open symbols) (mean ± one standard deviation; $n = 2$–5 for copepods or 5–12 for models).

3.2. Effect of morphology on the transition between non-leaky and leaky performance

Fluid velocity (U_{rel}) through a model M2 divided by the model's speed (U_{M2}) at that position is a measure of leakiness: high $U_{\mathrm{rel}}/U_{\mathrm{M2}}$ indicates sieve-like performance and low $U_{\mathrm{rel}}/U_{\mathrm{M2}}$ indicates paddle-like performance. We measured a transition between slightly leaky paddle-like behavior (i.e., fluid moved through the array of hairs much more slowly than the array was moving) and leaky, sieve-like performance as *Re* changed for the M2 models of all three species (Fig. 2). However, the *Re* range in which the transition in leakiness occurred was higher for the finely meshed M2's of *T. stylifera* than for the more coarsely meshed M2's of the other species.

A change in Re can be caused by a behavioral shift in M2 speed or by a change in seta diameter. Our models revealed that the morphology of a hairy appendage determines the Re range in which its leakiness is sensitive to such speed or size changes (Fig. 4). We found that the aspect of M2 structure that correlated with *Re*-sensitivity was the width of the gap between setules (G) relative to the size of the appendage (seta length, L). The finely meshed (low G/L) M2's of *T. stylifera* were insensitive to size or speed changes at low *Re*'s (10^{-2}–10^{-1}). In contrast, the leakiness of the coarser *C. velificatus* M2's (high G/L) was very sensitive

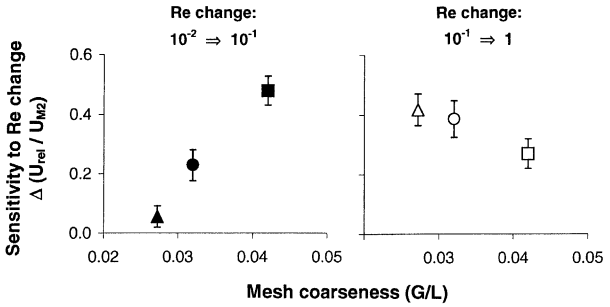

Fig. 4. Sensitivity to a 10-fold change in Reynolds number ($\Delta[U_{rel}/U_{M2}]=[\{U_{rel}/U_{M2}\}_{higher\ Re}]-[\{U_{rel}/U_{M2}\}_{lower\ Re}]$) plotted as a function of mesh coarseness (G/L) for the section of each model $0.25L$–$0.50L$ from the seta tip (L = seta length). Sensitivities of the M2's of *T. stylifera* (triangles), *E. pileatus* (circles), and *C. velificatus* (squares) are shown for *Re* changes from 10^{-2} to 10^{-1} (black symbols), and from 10^{-1} to 1 (open sysbols) (mean ± one standard deviation; $n=5$–12). Sensitivities of species differed significantly (ANOVA, SNK, $p<0.05$), except *T. stylifera* and *E. pileatus* for *Re* changing 10^{-1}–1.

to *Re* changes in this same low range (10^{-2}–10^{-1}). Conversely, we found that the finely meshed models were more sensitive to such changes than were the coarse ones at higher *Re*'s between 10^{-1} and 1.

4. Discussion

4.1. Leakiness of M2's determines mechanisms of food capture used by copepods

The *Re* at which the setae of the M2's of various species of copepods operate differs between species. The physical models used in this study revealed that the leakiness of the mesh of setae and setules on copepod M2's depends on *Re*. High-speed microcinematography of the motion of dye near real M2's capturing algal cells revealed how the leakiness of the M2's affects how algal cells are captured by different species of copeods (Koehl, 1992; Koehl and Strickler, 1981; Koehl and Paffenhofer, unpubl. data). We found that *E. pileatus* and *T. stylifera* M2's operate at setal *Re*'s of order 10^{-2} and act like slightly leaky paddles. Both *E. pileatus* and *T. stylifera* capture algal cells as the paddle-like M2's move apart from each other during the "fling" and draw water containing the particles towards the mouth. In contrast, the M2's of *C. velificatus* operate at setal *Re*'s of 1 and function like leaky sieves. The leaky M2's of *C. velificatus* capture algal cells by filtering them from the water as they move back towards each other during the "squeeze". Thus, copepods whose M2's function at *Re*'s lower than the *Re* range at which the transition in leakiness occurs capture particles by a different physical mechanism than do those whose M2's operate at *Re*'s above the transition.

Selective feeding by copepods can have important effects on phytoplankton community structure and copepod population dynamics (e.g. Donaghay, 1988; Frost, 1980; Hansen et al., 1994; Kleppel, 1993; Paffenhöfer, 1988). *E. pileatus* use different M2 motions when capturing large versus small algal cells (M2 *Re*'s of 8×10^{-2} and 2×10^{-2}, respectively) and when rejecting unwanted material (*Re* of 2×10^{-1}) (Koehl, 1992, 1995, 2001a; Koehl and Strickler, 1981; Koehl and Paffenhofer, unpubl. data). Our model measurements indicated that the flow through *E. pileatus* M2's should be sensitive to speed changes in this *Re* range, as corroborated by measurements of dye flow through the real M2's of feeding *E. pileatus* (Fig. 3). Thus, this species operates its M2's in a *Re* range where, simply by changing speed, it can switch between paddle-like function (moving food-containing parcels of water using slightly leaky M2's) (Koehl, 1995; Koehl and Strickler, 1981; Price and Paffenhöfer, 1984, 1986; Price et al., 1983) and sieve-like function (shoving unwanted material away from itself by passing water through leakier, rake-like M2's) (Koehl, 1995, 2001a; Koehl and Strickler, 1981).

4.2. Morphology determines sensitivity to changes in appendage speed

The finely meshed (low G/L) M2's of *T. stylifera* were insensitive to size or speed changes at low setal *Re*'s (10^{-2}–10^{-1}), hence this species should have permission in this *Re* range for behavioral changes and growth without alteration in the physical mechanism used to catch particles. In contrast, the leakiness of the coarser *C. velificatus* M2's (high G/L) was very sensitive to *Re* changes in this same low range (10^{-2}–10^{-1}). If the leakiness of a coarse array of hairs is altered by a change in *Re* from 10^{-2} to 10^{-1}, then novel mechanisms of operation can occur (e.g. a paddle can become a filter) due to simple changes in the speed or size of the appendage. Conversely, at higher *Re*'s between 10^{-1} and 1, the leakiness of finely meshed appendages is more sensitive to changes in size or speed than is that of coarse ones.

Our finding that the sensitivity of a hair-bearing appendage to size or speed changes depends on its mesh coarseness should shed light on how this important class of structures (that perform critical biological functions for so many animals in different phyla) interact with the fluid they process. For example, diverse arthropods have olfactory antennae or antennules bearing sensory hairs that operate in the *Re* range at which the leakiness transition occurs for their particular hair spacings. Therefore, when a crustacean flicks its antennules through the water or a moth fans air onto its antennae by flapping its wings, the increase in *Re* causes penetration of odor-bearing water or air into the array

of sensory hairs, i.e. the animal "sniffs" (Crimaldi et al., 2002; Goldman and Koehl, 2001; Koehl, 1996b, 2001b; Koehl et al., 2001; Loudon and Koehl, 2000; Mead and Koehl, 2000; Stacey et al., 2002).

Our models illustrate the general principle that a simple change in size (through ontogeny of an individual or evolution of a lineage) can sometimes result in a novel function (Kingsolver and Koehl, 1985; Koehl, 1996a) (in this case, a paddle can become a filter). They also illustrate the principle that there are size ranges in which the morphology of a structure makes little difference to its performance (Koehl, 1996a). These principles can be applied in studies of issues such as the evolution of feeding mechanisms in copepods, or the ontogeny of crustacean larvae as they molt to larger size and to new body designs.

Acknowledgements

I thank J. Jed for technical assistance and G.-A. Paffenhofer for collaboration in filming living copepods in his laboratory at the Skidaway Institute of Oceanography. This research was supported by grants from the National Science Foundation (#OCE-9907120 and #OCE-8917404).

References

Alexander, R.M., 1968. Animal Mechanics. University of Washington Press, Seattle.

Cheer, A.Y.L., Koehl, M.A.R., 1987a. Fluid flow through filtering appendages of insects. IMA Journal of Mathematics Applied in Medicine and Biology 4, 185–199.

Cheer, A.Y.L., Koehl, M.A.R., 1987b. Paddles and rakes: fluid flow through bristled appendages of small organisms. Journal of Theoretical Biology 129, 17–39.

Crimaldi, J.P., Koehl, M.A.R., Koseff, J.R., 2002. Effects of the resolution and kinematics of olfactory appendages on the interception of chemical signals in a turbulent odor plume. Environmental Fluid Mechanics 2, 35–63.

Dickinson, M.H., Farley, C.T., Full, R.J., Koehl, M.A.R., Kram, R., Lehman, S., 2000. How animals move: an integrative view. Science 288, 100–106.

Donaghay, P.L., 1988. Role of temporal scales of acclimation, food quality and trophic dominance in controlling the evolution of copepod feeding behavior. Bulletin of Marine Science 43, 469–485.

Frost, B.W., 1980. Grazing. In: Morris, I. (Ed.), The Physiological Ecology of Phytoplankton. University of California Press, Berkeley, CA, pp. 465–492.

Goldman, J.A., Koehl, M.A.R., 2001. Fluid dynamic design of lobster olfactory organs: high-speed kinematic analysis of antennule flicking by *panulirus argus*. Chemical Senses 26, 385–398.

Hansen, B., Bjørnsen, P.K., Hansen, P.J., 1994. The size ratio between planktonic predators and their prey. Limnology and Oceanography 39, 395–403.

Harris, R.P., 1996. Feeding ecology of Cananus. Ophelia 44, 85–109.

Itoh, K., 1970. A consideration on feeding habits of planktonic copepods in relation to the structure of their oral parts. Bulletin of the Plankton. Society of Japan 17, 1–10.

Kingsolver, J.G., Koehl, M.A.R., 1985. Aerodynamics, thermoregulation, and the evolution of insect wings: differential scaling and evolutionary change. Evolution 39, 488–504.

Kleppel, G.S., 1993. On the diets of calanoid copepods. Marine Ecology Progress Series 99, 183–195.

Koehl, M.A.R., 1984. Mechanisms of particle capture by copepods at low Reynolds numbers: possible modes of selective feeding. In: Meyers, D.G., Strickler, J.R. (Eds.), Trophic Dynamics Within Aquatic Ecosystems. Westview Press, Boulder, CO, pp. 135–166.

Koehl, M.A.R., 1992. Hairy little legs: Feeding, smelling, and swimming at low Reynolds number. Contemporary Mathematics 141, 33–64.

Koehl, M.A.R., 1995. Fluid flow through hair-bearing appendages: feeding, smelling, and swimming at low and intermediate reynolds number. In: Ellington, C.P., Pedley, T.J. (Eds.), Biological Fluid Dynamics. The Company of Biologists, Ltd, Cambridge, pp. 157–182.

Koehl, M.A.R., 1996a. When does morphology matter. Annual Review of Ecology and Systematics 27, 501–542.

Koehl, M.A.R., 1996b. Small-scale fluid dynamics of olfactory antennae. Marine and Freshwater Behavior and Physiology 27, 127–141.

Koehl, M.A.R., 1998. Small-scale hydrodynamics of feeding appendages of marine animals. Oceanography 11, 10–12.

Koehl, M.A.R., 1999. Ecological biomechanics: life history, mechanical design, and temporal patterns of mechanical stress. Journal of Experimental Biology 202, 3469–3476.

Koehl, M.A.R., 2001a. Transitions in function at low Reynolds number: hair-bearing animal appendages. Mathematical Methods in the Applied Sciences 24, 1523–1532.

Koehl, M.A.R., 2001b. Fluid dynamics of animal appendages that capture molecules: arthropod olfactory antennae. In: Fauci, L.J., Gueron, S. (Eds.), Computational Modeling in Biological Fluid Dynamics. Springer, New York, pp. 97–116.

Koehl, M.A.R., 2003. Physical modelling in biomechanics. Philosophical Transactions of the Royal Society of London B Biological Sciences 358, 1589–1596.

Koehl, M.A.R., Strickler, J.R., 1981. Copepod feeding currents: food capture at low reynolds number. Limnology and Oceanography 26, 1062–1073.

Koehl, M.A.R., Koseff, J.R., Crimaldi, J.P., McCay, M.G., Cooper, T., Wiley, M.B., Moore, P.A., 2001. Lobster sniffing: antennule design and hydrodynamic filtering of information in an odor plume. Science 294, 1948–1951.

Loudon, C., Koehl, M.A.R., 2000. Sniffing by a silkworm moth: wing fanning enhances air penetration through and pheromone interception by antennae. Journal of Experimental Biology 203, 2977–2990.

Loudon, C., Best, B.A., Koehl, M.A.R., 1994. When does motion relative to neighboring surfaces alter the flow through an array of hairs? Journal of Experimental Biology 193, 233–254.

Mead, K.S., Koehl, M.A.R., 2000. Stomatopod antennule design: the asymmetry, sampling efficiency, and ontogeny of olfactory flicking. Journal of Experimental Biology 203, 3795–3808.

Naganuma, T., 1996. Calanoid copepods: linking lower-higher trophic levels by linking lower-higher reynolds numbers. Marine Ecology Progress Series 136, 311–313.

Niklas, K.J., 1992. Plant Biomechanics: An Engineering Approach to Plant Form and Function. University of Chicago Press, Chicago.

Paffenhöfer, G.-A., 1988. Feeding rates and behavior of zooplankton. Bulletin of Marine Science 43, 430–435.

Price, H.J., Paffenhöfer, G.-A., 1984. Effects of feeding experience on the copepod *Eucalanus pileatus*: a cinematographic study. Marine Biology 84, 35–40.

Price, H.J., Paffenhöfer, G.-A., 1986. Capture of small cells by the copepod *Eucalanus elongatus*. Limnology and Oceanography 31, 189–194.

Price, J.H., Paffenhöfer, G.-A., Strickler, J.R., 1983. Modes of cell capture in calanoid copepods. Limnology and Oceanography 28, 116–123.

Rubenstein, D.I., Koehl, M.A.R., 1977. The mechanisms of filter feeding: some theoretical considerations. American Naturalist 111, 981–994.

Stacey, M.T., Mead, K.S., Koehl, M.A.R., 2002. Molecule capture by olfactory antennules: mantis shrimp. Journal of Mathematical Biology 44, 1–30.

Vogel, S., 1994. Life in Moving Fluids. Princeton University Press, Princeton, NJ.

Wainwright, P.C., Reilly, S.M. (Eds.), 1994. Ecological Morphology: Integrative Organismal Biology. University of Chicago Press, Chicago.

Wainwright, S.A., Biggs, W.D., Currey, J.D., Gosline, J.W., 1976. Mechanical Design in Organisms. Princeton University Press, Princeton.

White, F.M., 1974. Viscous Fluid Flow. McGraw Hill, New York.